

# Association of Retinal Sensitivity With Optical Coherence Tomography Microstructure in Highly Myopic Patients

Un Chul Park, Chang Ki Yoon, Kunho Bae, and Eun Kyung Lee

Department of Ophthalmology, Seoul National University College of Medicine, Seoul, Korea

Correspondence: Un Chul Park, Department of Ophthalmology, Seoul National University College of Medicine, 103 Daehak-ro, Jongno-gu, Seoul 110-799, Korea; [ucpark@snu.ac.kr](mailto:ucpark@snu.ac.kr).

Received: March 18, 2022

Accepted: September 6, 2022

Published: October 18, 2022

Citation: Park UC, Yoon CK, Bae K, Lee EK. Association of retinal sensitivity with optical coherence tomography microstructure in highly myopic patients. *Invest Ophthalmol Vis Sci.* 2022;63(11):13. <https://doi.org/10.1167/iovs.63.11.13>

**PURPOSE.** To investigate the association of retinal sensitivity with microstructural features in optical coherence tomography (OCT) of high myopic eyes.

**METHODS.** This cross-sectional study included 78 eyes (78 patients). Microstructural features on spectral-domain OCT, such as the integrity of the retinal pigment epithelium (RPE), ellipsoid zone (EZ), and external limiting membrane (ELM) and outer retinoschisis, were evaluated at each retinal location corresponding to microperimetric testing points.

**RESULTS.** For all testing points, retinal sensitivity was significantly associated with the integrity of the RPE, EZ, and ELM (all  $P < 0.001$ ) based on OCT but not with outer retinoschisis ( $P = 0.183$ ). A higher category of myopic maculopathy according to the Meta-Analysis of Pathologic Myopia classification was associated with lower mean retinal sensitivity ( $P < 0.001$ ). In eyes with patchy atrophy (PA), mean retinal sensitivity of testing points adjacent to the PA lesion ( $15.7 \pm 6.8$  dB) was greater than points within or at the PA border ( $2.6 \pm 5.2$  dB;  $P < 0.001$ ) but lower than distant points ( $19.6 \pm 4.3$  dB;  $P < 0.001$ ). Microstructural features in OCT were well correlated with the differences in retinal sensitivity according to myopic maculopathy severity and proximity to the PA lesion.

**CONCLUSIONS.** In highly myopic eyes, retinal sensitivity on microperimetry was strongly associated with microstructural features in OCT. Both retinal sensitivity and microstructure were affected by the severity of myopic degeneration and proximity to the PA lesion.

**Keywords:** high myopia, microperimetry, retinal sensitivity, pathologic myopia, microstructure

High myopia is one of the leading causes of irreversible visual impairment worldwide, especially in East Asia.<sup>1-3</sup> Maculopathy in highly myopic eyes has various clinical manifestations, and vision impairment usually results from pathologic changes of the macula such as chorioretinal atrophic change, retinoschitic change due to traction, and myopic macular neovascularization (MNV).<sup>4</sup> These atrophic, tractional, and neovascular components of myopic maculopathy are associated with microstructural changes in the macula, which can be observed in detail using optical coherence tomography (OCT). The progressive and continuous choroidal thinning observed in OCT plays a key role in diffuse chorioretinal atrophy,<sup>5</sup> whereas development of Bruch's membrane defect is a pathognomonic finding of patchy chorioretinal atrophy.<sup>6,7</sup> In addition, OCT examination is essential to establish the diagnosis of myopic retinoschisis, which is characterized in most cases by a splitting of the outer retinal layers.<sup>8</sup> In eyes with myopic MNV, subsequent development of MNV-related macular atrophy and subretinal fibrosis is also associated with defects in Bruch's membrane, retinal pigment epithelium (RPE), and photoreceptors.<sup>9,10</sup>

When assessing macular function, fundus-related microperimetry has the advantage of allowing simultaneous imaging of the fundus while projecting light stimuli onto a testing point. Precise topographical evaluation of

retinal sensitivity at a specific point enables the generation of a retinal sensitivity map registered with a fundus image. Previously, evaluation of the structure-function correlation by point-to-point matching of the retinal sensitivity map of microperimetry to OCT imaging has been performed in various retinal diseases such as neovascular age-related macular degeneration,<sup>11</sup> geographic atrophy,<sup>12</sup> macular telangiectasia,<sup>13</sup> diabetic retinopathy,<sup>14</sup> and retinitis pigmentosa.<sup>15</sup> In myopic maculopathy, the pathogenesis of which can involve one or more components of atrophy, traction, and neovascularization, analysis of the structure-function correlation may improve our understanding of the underlying pathophysiology. The present study evaluated the correlation of microstructural changes in OCT with retinal sensitivity in highly myopic patients.

## METHODS

### Study Population

This cross-sectional study reviewed the medical records of highly myopic patients consecutively examined by using spectral-domain OCT (SD-OCT) and microperimetry at the Pathologic Myopia Clinic of the Seoul National University Hospital between February 2020 and June 2020. The protocol and study design were approved by the Institutional

Review Board of Seoul National University Hospital (IRB no. 2003-231-1115), and the study was conducted in accordance with the tenets of the Declaration of Helsinki. High myopia was defined as an axial length of  $\geq 26.5$  mm or a myopic refractive error of  $\geq -6.0$  diopters. The exclusion criteria were (1) poor quality of SD-OCT image; (2) poor cooperation with the microperimetry examination, such as unstable fixation; (3) significant media opacities precluding fundus observation; (4) macular pathologic conditions other than high myopia; (5) active myopic MNV; (6) prior history of vitrectomy; or (7) prior diagnosis of glaucoma.

### Clinical Examination

All patients underwent a comprehensive ophthalmic examination including best-corrected visual acuity (BCVA), slit-lamp examination, dilated fundus examination, refractive error (spherical equivalent), axial length measurement, and ultra-widefield retinal imaging. Axial length measurements were performed by ocular biometry (IOLMaster; Carl Zeiss Meditec, Jena, Germany), and the ultra-widefield retinal image was taken with an Optos 200Tx Scanning Laser Ophthalmoscope (Optos PLC, Dunfermline, UK) centered on the macula. Based on ultra-widefield retinal imaging, myopic maculopathy was classified into four categories according to the Meta-Analysis of Pathologic Myopia (META-PM) Study Group classification: category 1, tessellated fundus; category 2, diffuse chorioretinal atrophy; category 3, patchy chorioretinal atrophy; and category 4, macular atrophy.<sup>16</sup> For patients in whom both eyes were eligible, only the eye with a higher category of myopic maculopathy was included for analysis in this study. If both eyes were of the same category, the eye with a longer axial length was chosen.

### Microperimetry

All patients were dilated with tropicamide 1% and phenylephrine 2.5% before microperimetry and SD-OCT examination. Retinal sensitivity measurements were performed using macular integrity assessment (MAIA) microperimetry (CenterVue, Padova, Italy) under mesopic conditions without dark adaptation. All patients underwent a quick training test to familiarize them with the procedure and to minimize the learning curve. Then, a standard expert test was performed using Goldmann III-sized stimuli projected against a white background with an illumination of 1.27 cd/m<sup>2</sup>. A standard 4-2 staircase strategy was used, with the stimuli ranging from 0 to 36 dB. A customized pattern with a grid consisting of 36 testing points in a 6 × 6 square centered on the fovea with 2° intervals between the adjoining rows and columns of testing points was used. Thus, rows or columns, each containing six testing points, were 1°, 3°, and 5° apart from both sides of the horizontal or vertical meridians passing through the central fovea (Figs. 1A, 1B). Hence, the testing points were approximately 1.4°, 3.2°, 4.3°, 5.1°, 5.8°, and 7.0° from the fovea. The fixation stability was assessed by the fixation index of P1 and P2, which represented the percentage of fixation points located within circles of 2° and 4° diameter, respectively. Fixation was considered “stable” when the P1 value was >75%, “relatively stable” when the P1 was <75% but P2 was >75%, and “unstable” when both P1 and P2 were <75%. The microperimetric results of patients who showed unstable fixation were excluded from the analysis. The testing points of microperimetry superimposed on the color fundus

images were graded into three zones based on their proximity to the patchy atrophy (PA) lesion. The testing points were graded as zone 1 if they fell within the PA lesion or at its border and as zone 2 if they were immediately adjacent to the testing points of zone 1. All other testing points, which were separated from the PA lesion by zone 2, were graded as zone 3. Regardless of PA, some nasal testing points that were located within the enlarged parapapillary atrophy (PPA) or adjacent to the PPA with distance of 2° or less were excluded from analysis.

### OCT Imaging and Structural Parameters

On the same day of microperimetry testing, SD-OCT (SPECTRALIS OCT; Heidelberg Engineering, Heidelberg, Germany) images were acquired with 37 horizontal raster scans covering an area of 15° × 15° centered on the fovea. The acquired OCT images were reviewed using Heidelberg Eye Explorer 1.10.2.0. The MAIA retinal sensitivity map image was superimposed onto the infrared image of the OCT to attain the highest correspondence using the retinal vessels as landmarks (Fig. 1C). In each eye, at 36 points in the infrared image of OCT corresponding to the 36 testing points by microperimetry, the retinal microstructure was graded for the following parameters: choroidal thickness (CT), outer retinal thickness (ORT), and presence of outer retinoschisis, as well as the integrity of the ellipsoid zone (EZ), external limiting membrane (ELM), and RPE. Using a caliper provided by the OCT machine, CT was measured manually as the perpendicular distance between the outer edge of the hyperreflective line of the RPE and the choroid-scleral junction, and ORT was measured between the inner edges of the outer plexiform layer and RPE. The OCT images were maximally magnified when the choroid was extremely thin; however, CT was recorded as 0 μm at points where the choroid was not visible. Outer retinoschisis was graded as present when splitting of the outer retinal layers, mainly between the outer plexiform and outer nuclear layer, was observed. The integrity of the EZ and RPE was graded as intact when the corresponding hyperreflective lines were fully visible, as disrupted when the lines were interrupted and only partially visible, or as absent. The ELM was graded as either intact or absent.

### Statistical Analysis

Two retinal specialists (CKY and EKL) performed the zone grading of microperimetry testing points and microstructural evaluation of the OCT B-scan images according to the definitions described above. Any discrepancies were adjudicated by a senior retinal specialist (UCP), and the CT and ORT measurements from the two graders were averaged for statistical analysis. The mean retinal sensitivity was compared according to the zone and category of myopic maculopathy using one-way ANOVA, and post hoc analysis was performed using the Bonferroni method. In addition, to identify factors associated with retinal sensitivity, univariable and multivariable mixed model analyses were performed. Only variables with  $P < 0.10$  by univariable analysis were included in the multivariable analysis. All statistical analyses were performed using SPSS Statistics 22.0 (IBM, Chicago, IL, USA), and  $P < 0.05$  was considered statistically significant.

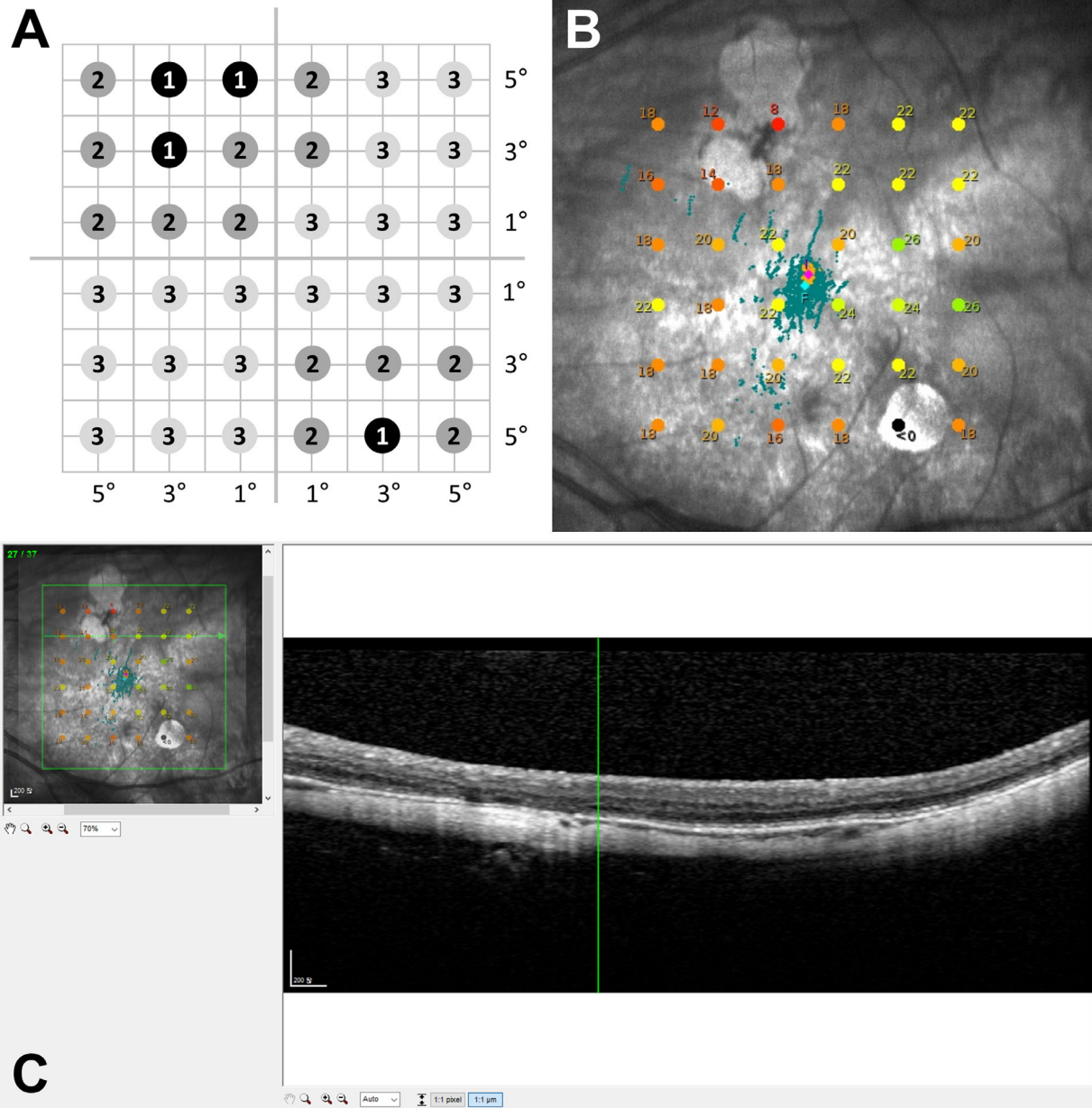


**FIGURE 1.** (A) Schematic illustration of a customized microperimetry sensitivity map comprised of 36 testing points. Each row or column contains six testing points 1°, 3°, and 5° apart from the horizontal or vertical meridians passing through the central fovea, generating a 6 × 6 square pattern centered on the fovea. The numbers indicate the designated zone for each testing point within the fundus image of (B) according to the proximity to the patchy atrophy lesion: zone 1, testing points within or at the border of patchy atrophy; zone 2, testing points immediately adjacent to the points designated as zone 1; and zone 3, all other testing points. (B) Representative fundus image of the microperimetry with the sensitivity values of each testing point presented in decibel units. (C) User interface for OCT to grade microstructural changes at the corresponding region to a stimulation point according to the superimposed translucent fundus image of microperimetry (B).

**RESULTS**

The analysis included 78 eyes of 78 patients with high myopia. The patient demographics and ocular characteristics are listed in Table 1. The mean age was 64.1 ± 10.0 years (range, 45-86), and the mean axial length was 30.0 ± 1.4 mm (range, 26.2–33.4). According to the META-PM Study Group classification, 14 eyes (17.9%), 33 eyes (42.3%), and 31 eyes (39.7%) were graded as having myopic maculopathy of category 1 (fundus tessellation), category 2 (diffuse

chorioretinal atrophy), and category 3 (patchy chorioretinal atrophy), respectively. Among 2808 testing points of 78 eyes in total, 27 in eyes without PA (category 1 or 2) and 71 in eyes with PA (category 3) were excluded from analysis because they were located within or adjacent to enlarged PPA. Thus, a total of 2710 testing points for retinal sensitivity were evaluated for their pointwise correlation to microstructural features based on B-scan images of the SD-OCT. The testing points designated as zone 1 (158 points, 5.8%) and zone 2



TABLE 1. Baseline Characteristics and Demographics of Patients

Parameters	Total	Category 1 (Fundus Tessellation)	Category 2 (Diffuse Atrophy)	Category 3 (Patchy Atrophy)	P*
Eyes, n (%)	78 (100.0)	14 (17.9)	33 (42.3)	31 (39.7)	
Age (y), mean ± SD (range)	64.1 ± 10.0 (45~86)	64.8 ± 10.7 (47~79)	61.3 ± 9.1 (45~83)	66.6 ± 10.1 (52~86)	0.101
Gender (female/male), n (%)	67 (85.9)/11 (14.1)	14(100.0)/0	27 (81.8)/5 (16.1)	26 (83.9)/5 (16.1)	0.324
Mean axial length (mm), mean ± SD (range)	30.0 ± 1.4 (26.2~33.4)	28.5 ± 1.1 (26.2~29.8)	29.8 ± 1.4 (27.1~32.2)	30.7 ± 1.1 (28.8~33.4)	<0.001
Presence of lacquer cracks, n (%)	24 (30.8)	1 (7.1)	13 (39.4)	10 (32.3)	0.095
History of myopic CNV, n (%)	15 (19.2)	0 (0.0)	7 (21.2)	8 (25.8)	0.123
Presence of posterior staphyloma, n (%)	48 (61.5)	7 (50.0)	21 (63.6)	20 (64.5)	0.649
BCVA (logMAR), mean ± SD (range; Snellen equivalent)	0.38 ± 0.30 (-0.18~1.70; 20/48)	0.34 ± 0.26 (0.15~2.50; 20/44)	0.37 ± 0.28 (-0.18~1.22; 20/47)	0.41 ± 0.33 (0.50~1.70; 20/51)	0.399
Macular sensitivity (dB), mean ± SD (range)†	18.8 ± 4.8 (2.7~26.8)	22.0 ± 2.7 (16.9~26.8)	19.9 ± 3.5 (7.9~25.6)	16.2 ± 5.4 (2.7~22.6)	<0.001
Choroidal thickness (µm), mean ± SD (range)†	29.6 ± 17.4 (5.4~84.9)	48.8 ± 12.0 (28.7~65.2)	32.3 ± 17.0 (11.0~84.9)	18.1 ± 9.6 (5.4~44.3)	<0.001
Outer retinal thickness (µm), mean ± SD (range)†	92.0 ± 21.5 (37.1~200.6)	98.7 ± 4.0 (90.4~105.2)	98.5 ± 25.7 (73.8~200.6)	82.0 ± 17.4 (37.1~120.7)	0.003
Testing points, n (%)	158 (5.8)	0 (0.0)	0 (0.0)	158 (15.1)	<0.001
Zone 1	219 (8.1)	0 (0.0)	0 (0.0)	219 (21.0)	
Zone 2	2333 (86.1)	501 (100.0)	1164 (100.0)	668 (63.9)	

\* One-way ANOVA.

† Mean and range of average of 36 testing points per eye.

(219 points, 8.1%) were distributed only in eyes graded as category 3.

The analysis of the B-scan images of OCT showed that the RPE line was intact at 2510 points (92.6%), disrupted at 68 points (2.5%), and absent at 139 points (5.1%), whereas the EZ line was intact at 2108 points (77.8%), disrupted at 316 points (11.7%), and absent at 286 points (10.6%). The ELM was intact at 2039 points (75.2%) and absent at 671 points (24.8%), and outer retinoschisis was present at 2547 points (94.0%) and absent at 163 points (6.0%). The retinal sensitivity results according to the microstructural features at each retinal location corresponding to the testing points of microperimetry are shown in Figure 2. The mean retinal sensitivities were significantly greater at testing points with intact RPE, EZ, or ELM lines compared to those in points where lines were disrupted or absent; moreover, testing points with disrupted lines had greater sensitivity compared to that in points where lines were absent (all  $P < 0.001$ ) (Figs. 2A–2C). However, the retinal sensitivities between testing points with and without outer retinoschisis did not differ ( $P = 0.183$ ) (Fig. 2D). For all testing points, retinal sensitivity was significantly correlated with outer retinal thickness ( $r = 0.352$ ,  $P < 0.001$ ) (Fig. 2E) and choroidal thickness ( $r = 0.295$ ,  $P < 0.001$ ) (Fig. 2F).

The retinal sensitivity of the testing points according to the categories of myopic maculopathy and zone distributions are shown in Figure 3. The mean retinal sensitivities of entire testing points in eyes with myopic maculopathy of categories 1, 2, or 3 were  $22.0 \pm 3.5$  dB,  $20.1 \pm 4.7$  dB, and  $16.2 \pm 7.8$  dB, respectively ( $F = 195.9$ ,  $P < 0.001$ ) (Fig. 3A). In subgroup analysis of eyes with category 3 myopic maculopathy, in which most of zones 1 and 2 testing points were included, the mean retinal sensitivities of the testing points designated as zones 1, 2, and 3 were  $2.6 \pm 5.2$  dB,  $15.7 \pm 6.8$  dB, and  $19.6 \pm 4.3$  dB, respectively ( $F = 719.4$ ,  $P < 0.001$ ) (Table 2). Post hoc analysis by the Bonferroni method revealed that the mean retinal sensitivity of testing points of zone 2 was greater than zone 1 ( $P < 0.001$ ) but lower than zone 3 ( $P < 0.001$ ). The hyperreflective lines of the RPE, EZ, and ELM were most frequently intact at points designated as zone 3 and least frequently intact at zone 1 testing points (all  $P < 0.001$ ). The frequency of outer retinoschisis did not differ according to the zone ( $P = 0.689$ ), and the presence of outer retinoschisis showed no significant association with RPE, EZ, and ELM integrity ( $P = 0.501$ ,  $P = 0.352$ , and  $P = 0.317$ , respectively).

The mean retinal sensitivities of the testing points designated as zones 1, 2, and 3 were  $2.6 \pm 5.2$  dB,  $15.7 \pm 6.8$  dB, and  $20.3 \pm 4.5$  dB, respectively ( $F = 1091.0$ ,  $P < 0.001$ ) (Fig. 3B). In the subgroup analysis of testing points of zone 3, the mean retinal sensitivities of zone 3 testing points in eyes with category 1, 2, or 3 myopic maculopathy were  $22.0 \pm 3.5$  dB,  $20.1 \pm 4.7$  dB, and  $19.6 \pm 4.3$  dB, respectively ( $F = 48.4$ ,  $P < 0.001$ ) (Table 2). Post hoc analysis showed that zone 3 testing points of eyes with category 1 myopic maculopathy had significantly greater retinal sensitivity compared to those of eyes with category 2 or 3 myopic maculopathy (corrected  $P < 0.001$  for both), but there was no difference between categories 2 and 3 (corrected  $P = 0.101$ ). Regarding the microstructural features, zone 3 testing points in eyes with a higher category of myopic maculopathy were less likely to have intact hyperreflective lines of the RPE, EZ, and ELM and more likely to have outer retinoschisis compared to zone 3 testing points in eyes with a lower category of myopic maculopathy ( $P \leq 0.001$ ).

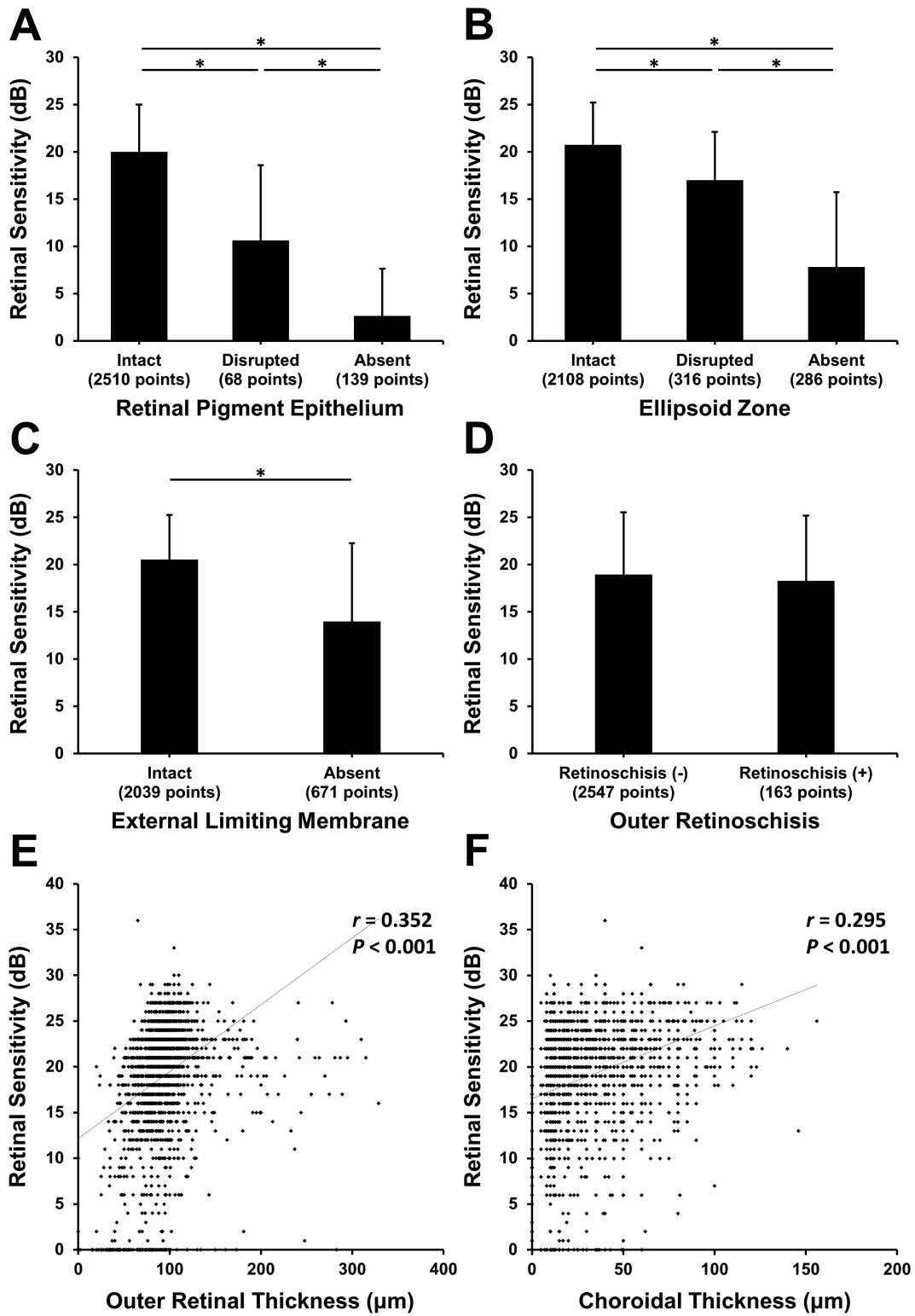


FIGURE 2. (A–D) Retinal sensitivity according to the integrity of hyperreflective lines of RPE (A), EZ (B), and ELM (C) and the presence of outer retinoschisis (D) on OCT. Asterisks indicate statistically significant differences. (E, F) Scattergrams showing the correlation of retinal sensitivity with ORT (E) and CT (F).

In consideration of the multiple testing points within an eye, mixed-model analysis was used to determine the factors associated with retinal sensitivity at a specific testing point. In multivariable analysis, which included all variables with

$P < 0.10$  in univariable analysis, older age, higher category of myopic maculopathy, location of testing points within or adjacent to PA lesion (zone 1 or 2), distance of testing points from the fovea, and absence or disruption of the RPE, EZ,

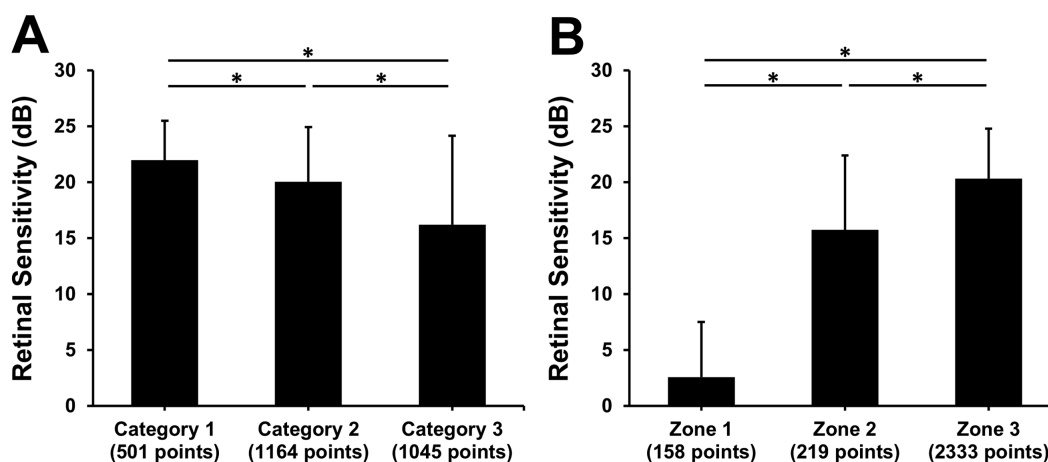


FIGURE 3. Retinal sensitivity according to the zone of testing points (A) and according to the category of myopic maculopathy (B). Asterisks indicate statistically significant differences.

TABLE 2. Subgroup Analysis of Retinal Sensitivity and Microstructural Changes on OCT for Eyes With Category 3 Myopic Maculopathy or for Testing Points Designated as Zone 3

	Category 3			P	Zone 3			P
	Zone 1 (158 Points)	Zone 2 (219 Points)	Zone 3 (668 Points)		Category 1 (501 Points)	Category 2 (1164 Points)	Category 3 (668 Points)	
Retinal sensitivity (dB), mean $\pm$ SD	2.6 $\pm$ 5.2	15.7 $\pm$ 6.8	19.6 $\pm$ 4.3	<0.001*	22.0 $\pm$ 3.5	20.1 $\pm$ 4.7	19.6 $\pm$ 4.3	<0.001*
RPE, n (%)				<0.001†				0.001†
Intact	12 (7.6)	188 (85.8)	653 (97.8)		501 (100)	1156 (99.3)	653 (97.8)	
Disrupted	24 (15.2)	23 (10.5)	13 (1.9)		0 (0)	8 (0.7)	13 (1.9)	
Absent	122 (77.2)	8 (3.7)	2 (0.3)		0 (0)	0 (0)	2 (0.3)	
EZ, n (%)				<0.001†				<0.001†
Intact	5 (3.2)	98 (44.7)	495 (74.1)		460 (91.8)	1050 (90.2)	495 (74.1)	
Disrupted	9 (5.7)	66 (30.1)	118 (17.7)		31 (6.2)	92 (7.9)	118 (17.7)	
Absent	144 (91.1)	55 (25.1)	55 (8.2)		10 (2.0)	22 (1.9)	55 (8.2)	
ELM, n (%)				<0.001†				<0.001†
Intact	14 (8.9)	109 (49.8)	479 (71.7)		421 (84.0)	1016 (87.3)	479 (71.7)	
Absent	144 (91.1)	110 (50.2)	189 (28.3)		80 (16.0)	148 (12.7)	189 (28.3)	
Outer retinoschisis, n (%)				0.689†				<0.001†
Retinoschitic change (–)	145 (91.8)	204 (93.2)	626 (93.7)		501 (100)	1071 (92.0)	626 (93.7)	
Retinoschitic change (+)	13 (8.2)	15 (6.8)	42 (6.3)		0 (0)	93 (8.0)	42 (6.3)	

\* One-way ANOVA.

†  $\chi^2$  test.

or ELM were significantly associated with decreased retinal sensitivity (Table 3).

## DISCUSSION

This cross-sectional study evaluated the association of retinal sensitivity in microperimetry with microstructural features in SD-OCT in highly myopic eyes. Point-to-point analysis revealed that greater retinal sensitivity was associated with more intact hyperreflective lines of the RPE and photoreceptor, and alterations in retinal function and microstructure were more frequently observed in eyes with higher category of myopic maculopathy. In eyes with PA lesion, retinal sensitivity within the PA was markedly decreased but showed gradual increase across the junctional zone, reflecting the difference in the integrity of the RPE and photoreceptors.

In this study, we adopted a customized map of a 6  $\times$  6 grid pattern to correlate testing points of microperimetry on the OCT raster scan images. Pointwise microstructural analysis of the OCT images showed that the integrity of the hyperreflective lines of RPE and photoreceptors as revealed by EZ and ELM were significantly associated with

retinal sensitivity, suggesting that these lines are important anatomical biomarkers of retinal function in myopic maculopathy. In addition, testing points were classified into three zones to assess retinal sensitivity according to the atrophic change of the retina and their proximity to the PA lesions. In eyes with PA lesions (namely, category 3 myopic maculopathy), the mean retinal sensitivity was lowest at zone 1 testing points, which were within or at the border of the PA lesion, followed by the adjacent points of zone 2 and distant points of zone 3, suggesting a gradual change in retinal sensitivity across the junctional zone of the PA lesion. These results imply that microperimetry is a useful functional assay to assess altered retinal function in patients with myopic maculopathy, particularly to detect scotoma and subtle functional decline around the atrophic lesion in patients with PA.<sup>17</sup> The completeness of hyperreflective lines of the RPE and photoreceptors in OCT also decreased gradually across the margin of PA lesions, reflecting the differences in retinal sensitivity among the zones. Thus, it could be concluded that anatomical and functional alterations also involve the adjacent region of the PA lesion, which significantly influences retinal sensitivity.

**TABLE 3.** Mixed Linear Regression Analyses to Determine Association of Retinal Sensitivity With Clinical and Microstructural Features on OCT

	Univariable Analysis		Multivariable Analysis	
	Coefficient (SE)	P	Coefficient (SE)	P
Age (y)	-0.150 (0.053)	0.006	-0.110 (0.035)	0.003
Gender (male vs. female)	-1.325 (1.588)	0.407	—	—
Axial length (mm)	-1.189 (0.368)	0.002	-0.112 (0.290)	0.700
Category of myopic maculopathy				
3 vs. 1	-6.179 (1.377)	<0.001	-2.295 (1.156)	0.049
2 vs. 1	-2.106 (1.364)	0.127	-2.377 (1.014)	0.022
Presence of posterior staphyloma	-1.182 (1.133)	0.300	—	—
Presence of lacquer crack	1.199 (1.195)	0.319	—	—
History of CNV treatment	-1.345 (1.400)	0.340	—	—
Zone				
1 vs. 3	-13.380 (0.434)	<0.001	-8.394 (0.605)	<0.001
2 vs. 3	-1.955 (0.329)	<0.001	-1.258 (0.310)	<0.001
Distance from fovea (°)	-0.609 (0.059)	<0.001	-0.507 (0.046)	<0.001
CT (μm)	0.019 (0.005)	<0.001	-0.004 (0.004)	0.316
ORT (μm)	0.044 (0.004)	<0.001	0.003 (0.003)	0.353
RPE				
Absent vs. intact	-11.896 (0.421)	<0.001	-2.144 (0.623)	0.001
Disrupted vs. intact	-5.654 (0.478)	<0.001	-1.122 (0.481)	0.020
EZ				
Absent vs. intact	-8.998 (0.313)	<0.001	-4.179 (0.359)	<0.001
Disrupted vs. intact	-2.572 (0.258)	<0.001	-1.465 (0.247)	<0.001
Absence of ELM	-3.536 (0.218)	<0.001	-0.946 (0.204)	<0.001
Presence of outer retinoschisis	-0.483 (0.504)	0.338	—	—

SE, standard error.

In contrast, in geographic atrophy due to age-related macular degeneration, which shows a funduscopy appearance similar to that of PA, retinal sensitivity was found to be abruptly decreased at the margins of atrophic lesions, whereas junctional zones adjoining the margins had sensitivity comparable to that of the uninvolved distant regions.<sup>18</sup> This is different from the gradual transition in anatomy and function observed in the present study. Although this discrepancy might have resulted from different microperimetric testing protocol between the studies, it might suggest differences in the pathophysiology underlying the development and progression of atrophic lesions between non-exudative age-related macular degeneration and pathologic myopia.

In the present study, the mean retinal sensitivity decreased significantly as the category of myopic maculopathy increased, indicating a more global function deficit in eyes with more severe myopic degeneration. Even between eyes with categories 1 and 2 myopic maculopathy, there was significant difference in retinal sensitivity. This finding suggests that subtle deterioration in retinal function may occur during the early stages of myopic maculopathy progression. Wang et al.<sup>19</sup> performed adaptive optics analysis in myopic eyes with good vision and found more decreased cone density in eyes with high myopia compared to that in eyes with low or moderate myopia, a finding that was significantly associated with decreased retinal sensitivity. With the axial elongation of the eyeball during myopia progression, retinal stretching may result in anatomical and functional alterations in the photoreceptors. Decreased melanin pigment distribution or deep vascular density in myopic eyes with greater axial length and their independent associations with reduced retinal sensitivity were observed in the previous studies,<sup>20,21</sup> and these also suggest the influ-

ence of eyeball stretching on the retinal sensitivity in high myopic eyes. Interestingly, although the mean retinal sensitivities were comparable between zone 3 testing points of eyes with category 2 or 3 myopic maculopathy, disruption or absence of RPE and photoreceptor lines was more frequently observed in zone 3 testing points of eyes with category 3 myopic maculopathy. This finding suggests that microstructural alterations may precede any functional decline in the uninvolved distant retinal region of eyes with PA.

The clinical implications of altered retinal sensitivity and microstructure in the retinal region not involved in PA lesions are unclear. In long-term cohort studies of highly myopic patients, more than half of the eyes with diffuse atrophy and almost all eyes with PA showed the progression of myopic maculopathy.<sup>22,23</sup> One can hypothesize that the retinal regions of zone 2 or 3 with decreased retinal sensitivity or impaired microstructure are more likely to develop into PA lesions either de novo or by enlargement of preexisting lesions in the future; however, further longitudinal studies are required to elucidate this possibility.

In this study, 6.0% of the total testing points showed outer retinoschisis on OCT. High myopic patients with foveoschisis reportedly have impaired vision compared to those without for various functional parameters, including retinal sensitivity<sup>24,25</sup>; however, the point-to-point analysis in the present study revealed no significant influence of outer retinoschisis on retinal sensitivity at the corresponding points. The reason for this finding is unclear but may be because the splitting of the outer retinal layer in this study was generally mild, without foveal detachment or macular hole. Weak stretching of Henle's nerve fiber, which is thought to represent the intraretinal columnar structure within the retinoschitic space,<sup>26</sup> may not have significantly impaired retinal sensitivity, although it contains axons of photoreceptors.<sup>27</sup>



Consistent with these findings, we observed no difference in RPE and photoreceptor integrity on OCT according to the presence of outer retinoschisis.

The present study has several limitations. First, this study was cross-sectional and did not provide any prognostic information on the progression of myopic maculopathy. A longitudinal study is needed to elucidate the predictive role of decreased retinal sensitivity in zone 2 on the progression of PA lesions and a more defined structure–function relationship in myopic maculopathy. Second, although we tried to match point-to-point based on fundus images, the microperimetry testing points may not exactly overlay the raster scans of OCT. However, the error would be less than 0.208°, considering an interval between two adjacent OCT horizontal scan lines. Third, this study did not analyze the influence of any inner retinal changes, such as inner retinoschisis or epiretinal membrane, due to the inability to calculate the displacement of ganglion cells from their receptive field. Fourth, microperimetry was performed only once per patient; hence, test–retest variability and the influence of a learning effect were not reflected in the results of this study. Finally, the influence of PPA on retinal sensitivity was not evaluated in this study. Although the fundusopic and OCT features are similar between the PPA and PA,<sup>6,28</sup> 98 testing points within or adjacent to PPA lesions were excluded from analysis considering their different mechanisms.

In summary, microperimetry is a useful functional assay to assess altered retinal function in patients with myopic maculopathy. Point-to-point analysis revealed that retinal sensitivity was strongly associated with the retinal microstructural changes in OCT. Alterations in retinal microstructure and function were different according to the severity of myopic degeneration and proximity to the PA lesion. Further longitudinal studies may be required to elucidate the implications of retinal sensitivity in the structure–function correlation and the progression of myopic maculopathy.

### Acknowledgments

Disclosure: U.C. Park, None; C.K. Yoon, None; K. Bae, None; E.K. Lee, None

### References

- Iwase A, Araie M, Tomidokoro A, Yamamoto T, Shimizu H, Kitazawa Y. Prevalence and causes of low vision and blindness in a Japanese adult population: the Tajimi Study. *Ophthalmology*. 2006;113(8):1354–1362, <https://doi.org/10.1016/j.ophtha.2006.04.022>.
- Xu L, Wang Y, Li Y, et al. Causes of blindness and visual impairment in urban and rural areas in Beijing: the Beijing Eye Study. *Ophthalmology*. 2006;113(7):1134.e1–1134.e11, <https://doi.org/10.1016/j.ophtha.2006.01.035>.
- Varma R, Kim JS, Burkemper BS, et al. Prevalence and causes of visual impairment and blindness in Chinese american adults the Chinese american eye study. *JAMA Ophthalmol*. 2016;134(7):785–793, <https://doi.org/10.1001/jamaophthalmol.2016.1261>.
- Ruiz-Medrano J, Montero JA, Flores-Moreno I, Arias L, García-Layana A, Ruiz-Moreno JM. Myopic maculopathy: current status and proposal for a new classification and grading system (ATN). *Prog Retin Eye Res*. 2019;69:80–115, <https://doi.org/10.1016/j.preteyeres.2018.10.005>.
- Fang Y, Du R, Nagaoka N, et al. OCT-based diagnostic criteria for different stages of myopic maculopathy. *Ophthalmology*. 2019;126(7):1018–1032, <https://doi.org/10.1016/j.ophtha.2019.01.012>.
- Du R, Fang Y, Jonas JB, et al. Clinical features of patchy chorioretinal atrophy in pathologic myopia. *Retina*. 2020;40(5):951–959, <https://doi.org/10.1097/iae.0000000000002575>.
- Ohno-Matsui K, Jonas JB, Spaide RF. Macular Bruch membrane holes in highly myopic patchy chorioretinal atrophy. *Am J Ophthalmol*. 2016;166:22–28, <https://doi.org/10.1016/j.ajo.2016.03.019>.
- Shinohara K, Tanaka N, Jonas JB, et al. Ultrawide-field OCT to investigate relationships between myopic macular retinoschisis and posterior staphyloma. *Ophthalmology*. 2018;125(10):1575–1586, <https://doi.org/10.1016/j.ophtha.2018.03.053>.
- Ahn SJ, Park KH, Woo SJ. Subretinal fibrosis after anti-vascular endothelial growth factor therapy in eyes with myopic choroidal neovascularization. *Retina*. 2016;36(11):2140–2149, <https://doi.org/10.1097/IAE.0000000000001043>.
- Ohno-Matsui K, Jonas JB, Spaide RF. Macular Bruch membrane holes in choroidal neovascularization-related myopic macular atrophy by swept-source optical coherence tomography. *Am J Ophthalmol*. 2016;162:133–139.e1, <https://doi.org/10.1016/j.ajo.2015.11.014>.
- Sulzbacher F, Kiss C, Kaider A, et al. Correlation of SD-OCT features and retinal sensitivity in neovascular age-related macular degeneration. *Invest Ophthalmol Vis Sci*. 2012;53(10):6448–6455, <https://doi.org/10.1167/iovs.11-9162>.
- Sayegh RG, Kiss CG, Simader C, et al. A systematic correlation of morphology and function using spectral domain optical coherence tomography and microperimetry in patients with geographic atrophy. *Br J Ophthalmol*. 2014;98(8):1050–1055, <https://doi.org/10.1136/bjophthalmol-2014-305195>.
- Sallo FB, Leung I, Clemons TE, et al. Correlation of structural and functional outcome measures in a phase one trial of ciliary neurotrophic factor in type 2 idiopathic macular telangiectasia. *Retina*. 2018;38(suppl 1):S27–S32, <https://doi.org/10.1097/IAE.0000000000001706>.
- Montesano G, Gervasoni A, Ferri P, et al. Structure-function relationship in early diabetic retinopathy: a spatial correlation analysis with OCT and microperimetry. *Eye (Lond)*. 2017;31(6):931–939, <https://doi.org/10.1038/eye.2017.27>.
- Funatsu J, Murakami Y, Nakatake S, et al. Direct comparison of retinal structure and function in retinitis pigmentosa by co-registering microperimetry and optical coherence tomography. *PLoS One*. 2019;14(12):1–13, <https://doi.org/10.1371/journal.pone.0226097>.
- Ohno-Matsui K, Kawasaki R, Jonas JB, et al. International photographic classification and grading system for myopic maculopathy. *Am J Ophthalmol*. 2015;159(5):877–883, <https://doi.org/10.1016/j.ajo.2015.01.022>.
- Lo J, Poon LYC, Chen YH, et al. Patchy scotoma observed in chorioretinal patchy atrophy of myopic macular degeneration. *Invest Ophthalmol Vis Sci*. 2020;61(2):15, <https://doi.org/10.1167/iovs.61.2.15>.
- Hariri AH, Tepelus TC, Akil H, Nittala MG, Sadda SR. Retinal sensitivity at the junctional zone of eyes with geographic atrophy due to age-related macular degeneration. *Am J Ophthalmol*. 2016;168:122–128, <https://doi.org/10.1016/j.ajo.2016.05.007>.
- Wang Y, Ye J, Shen M, et al. Photoreceptor degeneration is correlated with the deterioration of macular retinal sensitivity in high myopia. *Invest Ophthalmol Vis Sci*. 2019;60(8):2800–2810, <https://doi.org/10.1167/iovs.18-26085>.
- Tsui CK, Yang B, Yu S, et al. The relationship between macular vessel density and thickness with light



- sensitivity in myopic eyes. *Curr Eye Res.* 2019;44(10):1104–1111, <https://doi.org/10.1080/02713683.2019.1627461>.
21. Harimoto A, Obata R, Yamamoto M, et al. Retinal pigment epithelium melanin distribution estimated by polarisation entropy and its association with retinal sensitivity in patients with high myopia [published online ahead of print May 6, 2021]. *Br J Ophthalmol*, <https://doi.org/10.1136/BJOPHTHALMOL-2021-318890>.
  22. Fang Y, Yokoi T, Nagaoka N, et al. Progression of myopic maculopathy during 18-year follow-up. *Ophthalmology*. 2018;125(6):863–877, <https://doi.org/10.1016/j.ophtha.2017.12.005>.
  23. Yan YN, Wang YX, Yang Y, et al. Ten-year progression of myopic maculopathy: the Beijing Eye Study 2001–2011. *Ophthalmology*. 2018;125(8):1253–1263, <https://doi.org/10.1016/j.ophtha.2018.01.035>.
  24. Li Q, Wang H, Gao P. Assessment of visual function in patients with myopic foveoschisis. *Curr Eye Res.* 2019;44(1):76–81, <https://doi.org/10.1080/02713683.2018.1516782>.
  25. Nebbioso M, Lambiase A, Gharbiya M, Bruscolini A, Alisi L, Bonfiglio V. High myopic patients with and without foveoschisis: morphological and functional characteristics. *Doc Ophthalmol.* 2020;141(3):227–236, <https://doi.org/10.1007/s10633-020-09767-y>.
  26. Curcio CA, Allen KA. Topography of ganglion cells in human retina. *J Comp Neurol.* 1990;300(1):5–25, <https://doi.org/10.1002/cne.903000103>.
  27. Lujan BJ, Roorda A, Knighton RW, Carroll J. Revealing Henle's fiber layer using spectral domain optical coherence tomography. *Invest Ophthalmol Vis Sci.* 2011;52(3):1486–1492, <https://doi.org/10.1167/iovs.10-5946>.
  28. Dai Y, Jonas JB, Huang H, Wang M, Sun X. Microstructure of parapapillary atrophy: beta zone and gamma zone. *Invest Ophthalmol Vis Sci.* 2013;54(3):2013–2018, <https://doi.org/10.1167/iovs.12-11255>.